



A deep learning-based model for the cross-scale instability in fusion plasmas

Hui Li,¹ Yanlin Fu,² Yifei Zhao,^{1,3} Lian Wang,³ Tianbo Wang,³
Zhengxiong Wang,¹ Jiquan Li,³

¹ Dalian University of Technology, Dalian, China

² Dalian Institute of Chemical Physics, Chinese Academy of Sciences, Dalian, China

³ Southwestern Institute of Physics, Chengdu, China

Workshop on Artificial Intelligence for Accelerating Fusion and Plasma Science

28 November – 1 December 2023, Vienna, Austria





1

Background & Motivation

2

Multi-mode interaction & Neural network

3

Multi-scale interaction & Neural network

4

Summary

CONTENT



1

Background & Motivation

2

Multi-mode interaction & Neural network

3

Multi-scale interaction & Neural network

4

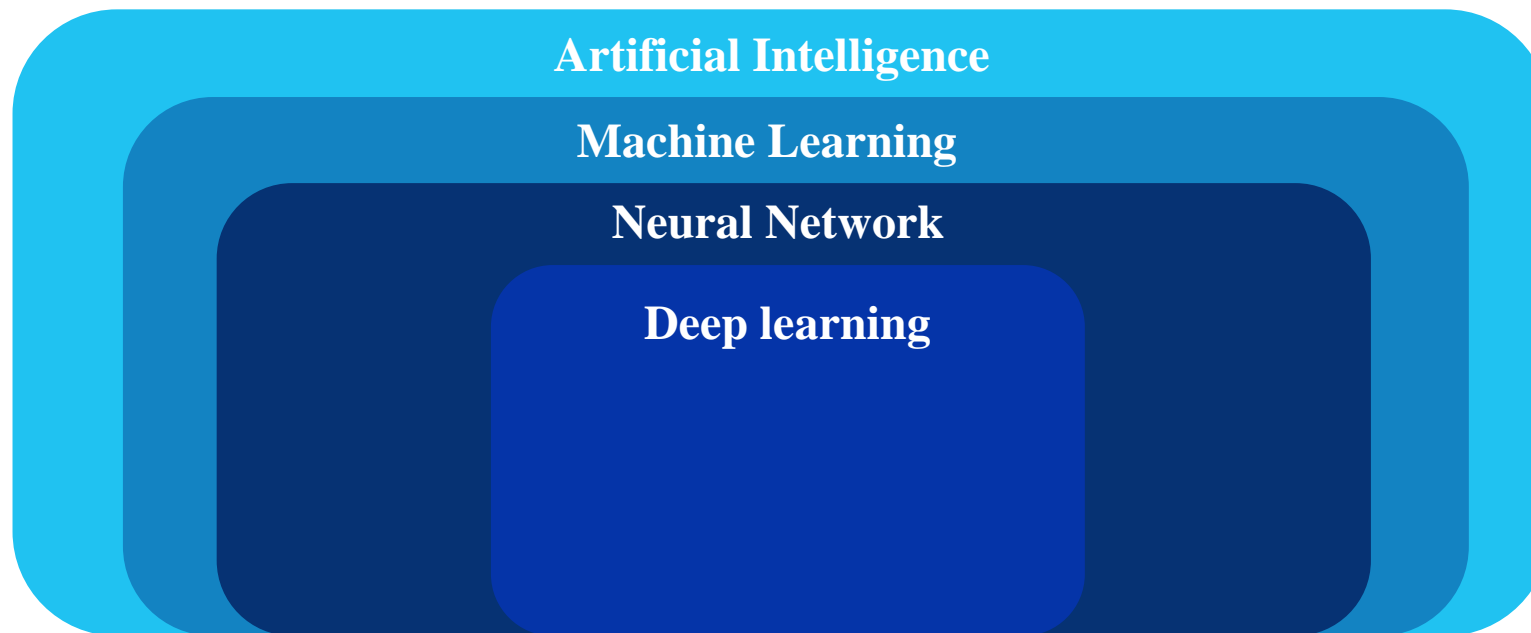
Summary

CONTENT

✓ Machine Learning .VS. Deep Learning. VS. Neural Network

Preparing for the future

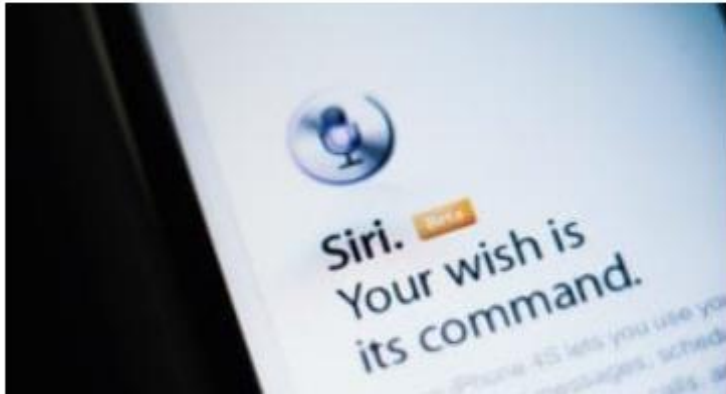
- **Machine learning: multi-field interdisciplinary.**
- **Neural Network: interconnected neurons adapt input value to corresponding output.**
- **Deep learning: advanced version of neural network.**



✓ Application for the deep learning

Preparing for the future

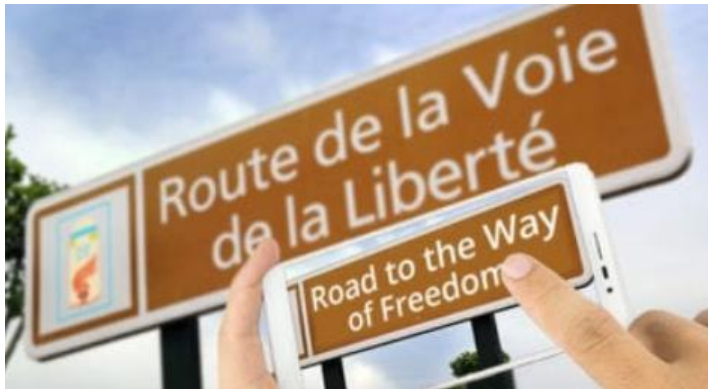
- Automatic Speech Recognition



- Automatic Machine Translation



- Image Recognition



- Autonomous vehicles





1

Background & Motivation

2

Multi-mode interaction & Neural network

3

Multi-scale interaction & Neural network

4

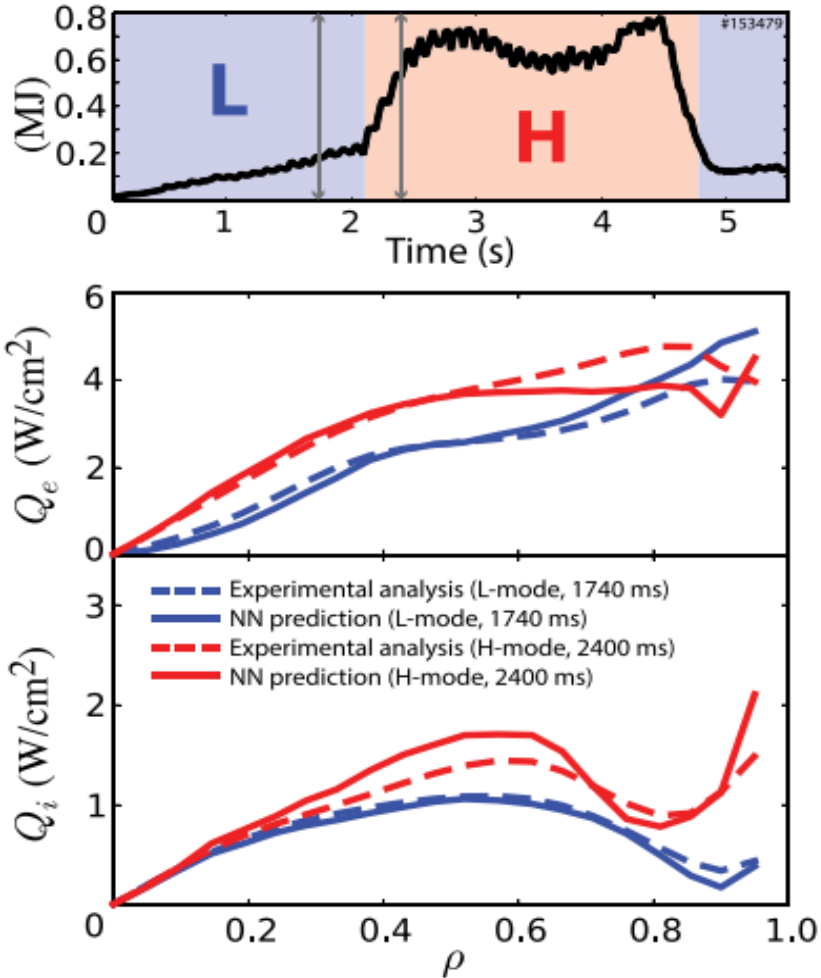
Summary

CONTENTS

✓ NN .VS. DIII-D Experiment

Preparing for the future

[Meneghini, et al. POP 21 (2014)]



• Input to the neural network

TABLE I. Local dimensionless plasma parameters which are input to the neural network.

r/a	→	Normalized minor radius
R/a	→	Normalized major radius
κ	→	Elongation
$r\dot{\kappa}$	→	Normalized elongation shear
δ	→	Triangularity
q	→	Safety factor
$r\dot{q}$	→	Normalized safety factor shear
$\nu_{ie}a/c_s$	→	Normalized electron-ion collision frequency
λ_d/a	→	Normalized Debye length
β_e	→	Kinetic to magnetic pressure ratio
ρ_i/a	→	Normalized ion gyroradius
v_{\parallel}/c_s	→	Normalized parallel velocity
$r\dot{v}_{\parallel}/c_s$	→	Normalized parallel velocity shear
$r\dot{v}_{\perp}/c_s$	→	Normalized $E \times B$ velocity shear
T_i/T_e	→	Ion to electron temperature ratio
n_i/n_e	→	Ion to electron density ratio
$a/ L_{Te} $	→	Electron temperature scale length
$a/ L_{Ti} $	→	Ion temperature scale length
$a/ L_{ne} $	→	Electron density scale length
$a/ L_{ni} $	→	Ion density scale length
$a/ L_p $	→	Total pressure scale length

- NN predictions of heat flux profiles .VS. measurements;
- Steady state and transients phases of L and H-mode regimes;
- Both are in good agreement.

FIG. 3. Sample comparison of the electron and ion heat flux profiles from the 2013 experimental campaign and predicted by the NN. The profiles predicted by the NN are smooth and agree well with the measurements across the whole plasma radius for both H and L plasma phases.

• Input parameters for the QuaLiKiz

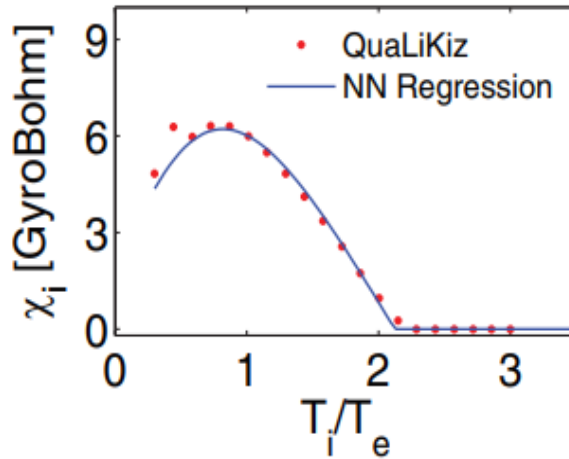
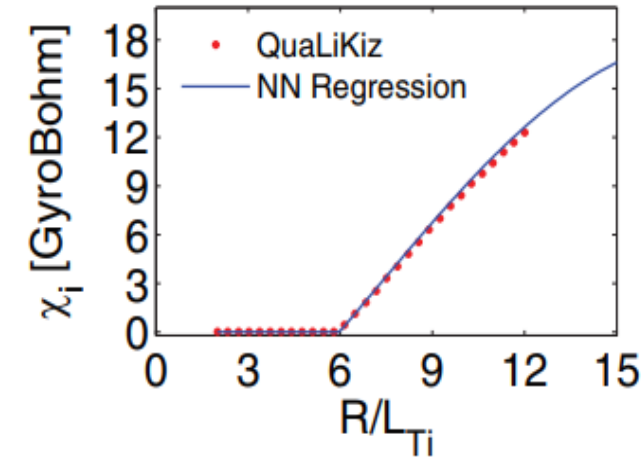
Table 1. Summary of input parameters for the QuaLiKiz adiabatic electron ITG database employed in this work.

Parameter	Min value	Max value	No. of points
R/L_{Ti}	2	12	30
T_i/T_e	0.3	3	20
q	1	5	20
\hat{s}	0.1	3	20
$k_{\theta}\rho_s$	0.05	0.8	16
Total no. of points			3 840 000

- **NN parameter scans;**
- **The typical quality of the fits;**
- **Implemented both in CRONOS and RAPTOR integrated modelling codes.**

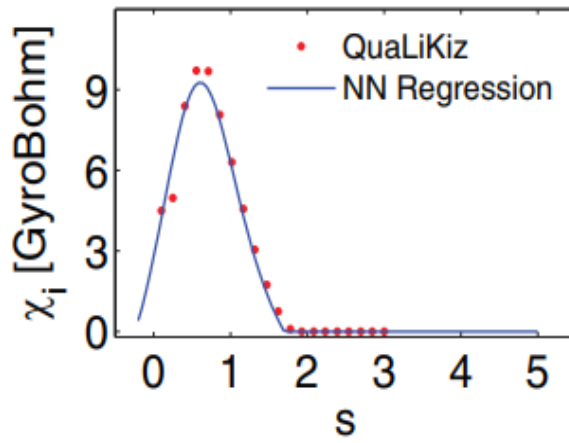
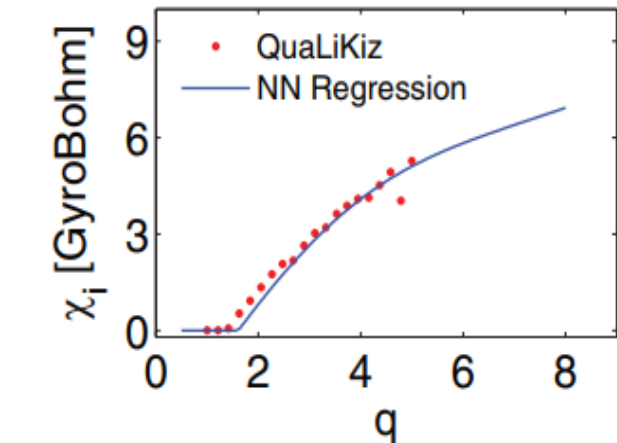
$T_i/T_e=1.29, s=0.86, q=1$

$R/L_{Ti}=8.21, s=0.86, q=1.42$



$R/L_{Ti}=6.48, T_i/T_e=0.87, s=1.32$

$R/L_{Ti}=8.21, T_i/T_e=1.15, q=2.05$



✓ 5-field electrostatic ITG model with trapped electron response

Preparing for the future

- **ExFC:** A fluid model-based framework for the simulation of flux-driven turbulence and global transport;
- **Configuration:** tokamak torus coordinates (r, θ, φ) ;
- **General modeling equations:** convection -diffusion equations with sources and sinks.

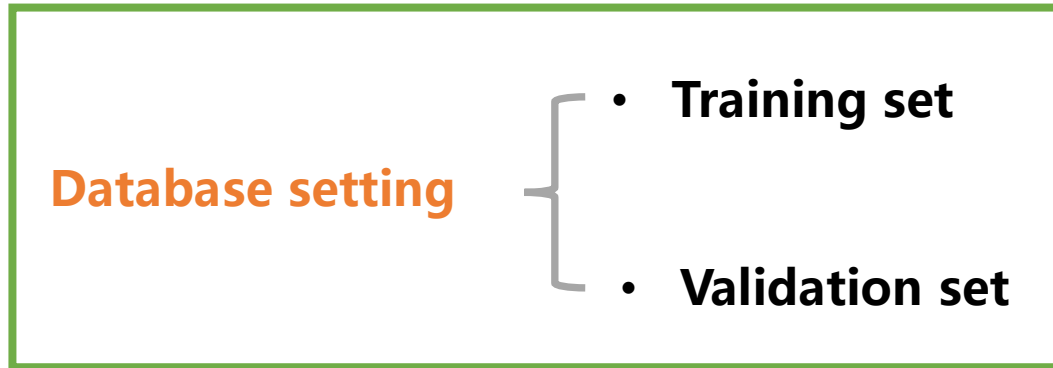
$$\frac{dn_e}{dt} = -\omega_{dte}(n_0\phi - T_{e0}n_e - n_0T_e) + D_n\nabla_{\perp}^2 n_e$$

$$\frac{dT_e}{dt} = -T_{e0}\omega_{dte}[(\Gamma - 1)(\phi + T_{e0}/n_0n_e) + (2\Gamma - 1)T_e] - (\Gamma - 1)\sqrt{(8m_eT_{e0})/(m_i\pi)}|\nabla_{\parallel}|T_e + D_{Te}\nabla_{\perp}^2 T_e$$

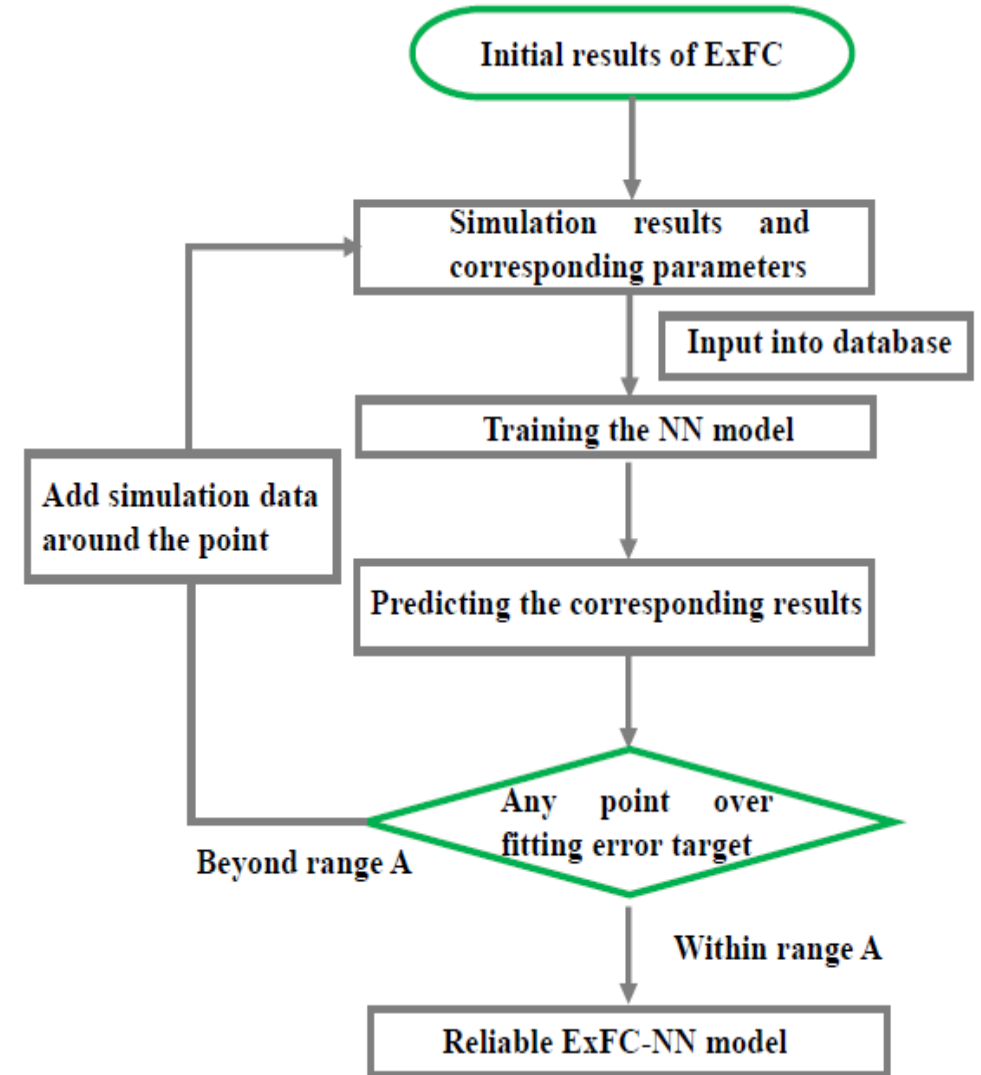
$$\begin{aligned} \frac{d\Omega}{dt} = & aT_{i0}(\nabla_r n_0/n_0 + \nabla_r T_{i0}/T_{i0})\nabla_{\theta}\nabla_{\perp}^2\phi + af_c\nabla_r n_0/n_0\nabla_{\theta}\phi - \nabla_{\parallel}v_{\parallel} + f_t\omega_{dte}(\phi - T_e - T_{i0}/n_0n_e) \\ & + \omega_d((1 + f_c)\phi + T_i + f_tT_{i0}/n_0n_e) + D_U\nabla_{\perp}^2\Omega \end{aligned}$$

$$\frac{dv_{\parallel}}{dt} = -\nabla_{\parallel}T_i - f_tT_{i0}/n_0\nabla_{\parallel}n - (1 + f_c)\nabla_{\parallel}\phi + D_v\nabla_{\perp}^2v_{\parallel}$$

$$\frac{dT_i}{dt} = -(\Gamma - 1)\nabla_{\parallel}v_{\parallel} + T_{i0}\omega_{di}[(\Gamma - 1)(f_c\phi + f_tT_{i0}/n_0n) + (2\Gamma - 1)T_i] - (\Gamma - 1)\sqrt{8T_{i0}/\pi}|\nabla_{\parallel}|T_i + D_{Ti}\nabla_{\perp}^2T_i$$



• Schematic diagram of ExFC-NN



Hui Li, J. Q. Li, Y. L. Fu, Z. X. Wang, *et al.*, *Nucl. Fusion* 62, 036014 (2022).

Hui Li, Y. L. Fu, J. Q. Li, Z. X. Wang., *Plasma Sci. Technol.* 23, 115102 (2021).



1

Background & Motivation

2

Multi-mode interaction & Neural network

3

Multi-scale interaction & Neural network

4

Summary

CONTENT

✓ A slab version of a 5-field Landau fluid model

Preparing for the future

LLF5

$$d_t \nabla_{\perp}^2 \phi = (1 + \eta_i) \partial^2 \phi + \nabla_{\parallel} j_{\parallel} + D_U \nabla_{\perp}^4 \phi$$

$$\beta \partial_t \Psi = \nabla_{\parallel} (\phi - n) + \beta (1 - v_0) \partial_y \Psi + \eta j_{\parallel} - \sqrt{\pi m_e / 2 m_i} |\nabla_{\parallel}| (v_{\parallel} - j_{\parallel})$$

$$d_t n = -\partial_y \phi - \nabla_{\parallel} v_{\parallel} + \nabla_{\parallel} j_{\parallel} + D_n \nabla_{\perp}^2 n$$

$$d_t v_{\parallel} = -2 \nabla_{\parallel} n - \nabla_{\parallel} T_i - \beta (2 + \eta_i) \partial_y \Psi + \eta_{\perp} \nabla_{\perp}^2 v_{\parallel}$$

$$d_t T_i = -\eta_i \partial_y \phi - \frac{2}{3} \nabla_{\parallel} v_{\parallel} - \frac{2}{3} \sqrt{8/\pi} |\nabla_{\parallel}| T_i + \chi_{\perp} \nabla_{\perp}^2 T_i$$

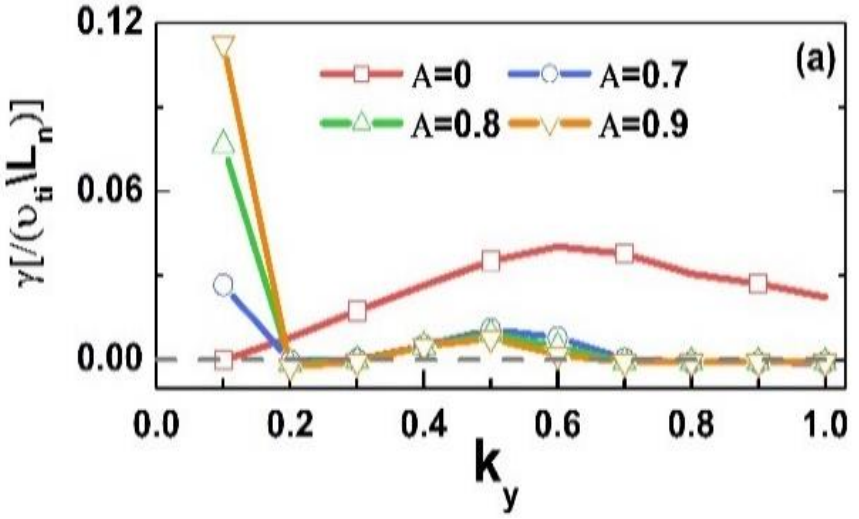
★ The externally imposed $\vec{E} \times \vec{B}$ shear flow

$$v_0 = A \sin(k_q x)$$

✓ Evolution of multi-scale instabilities

Preparing for the future

• Linear growth rates

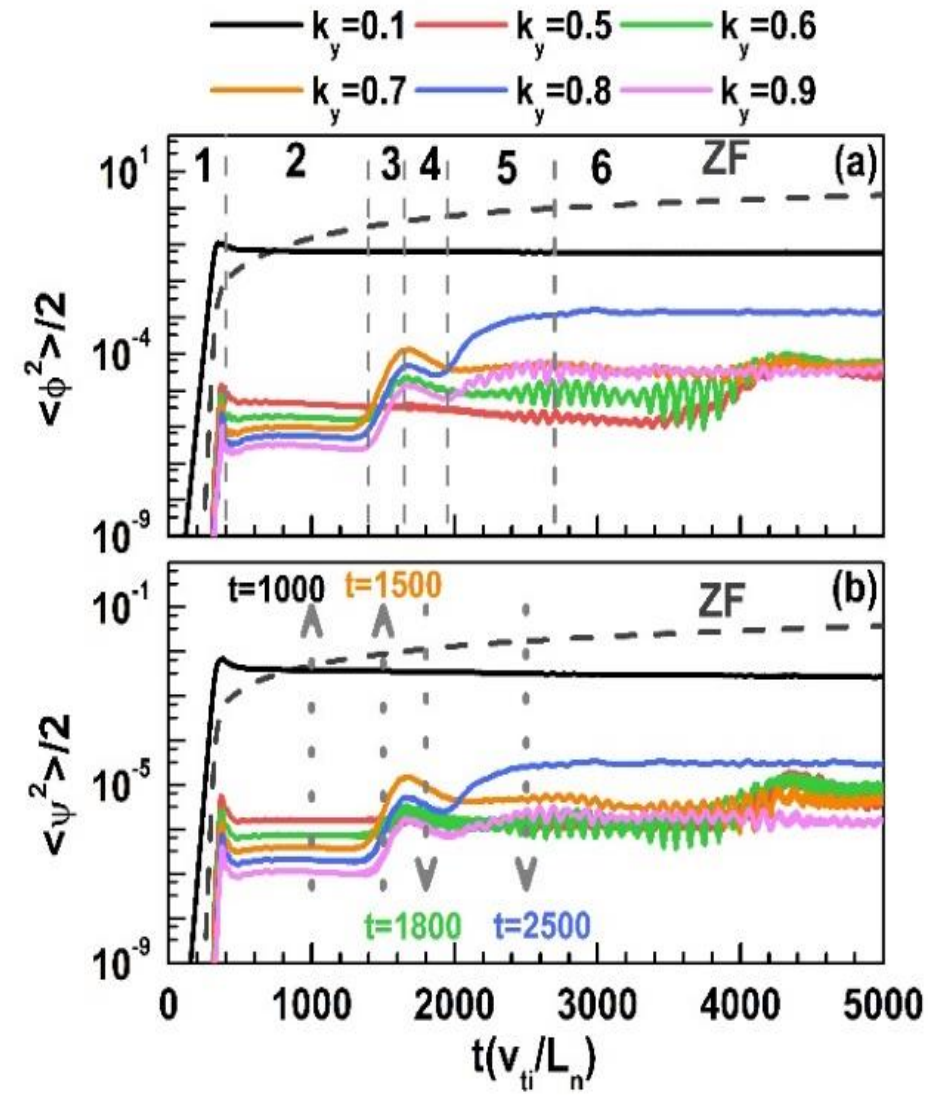


Mode coupling between multi-scale modes

Spectrum

• Zonal flow & KH instability & ITG instability

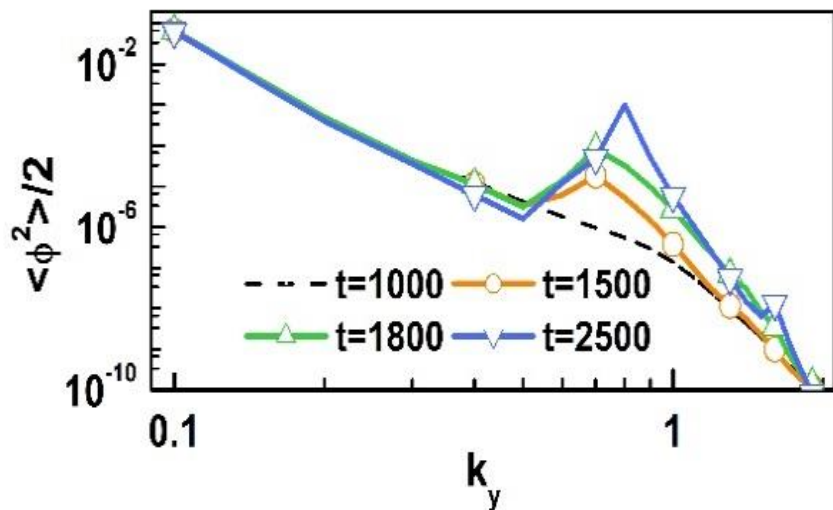
($A = 0.72$)



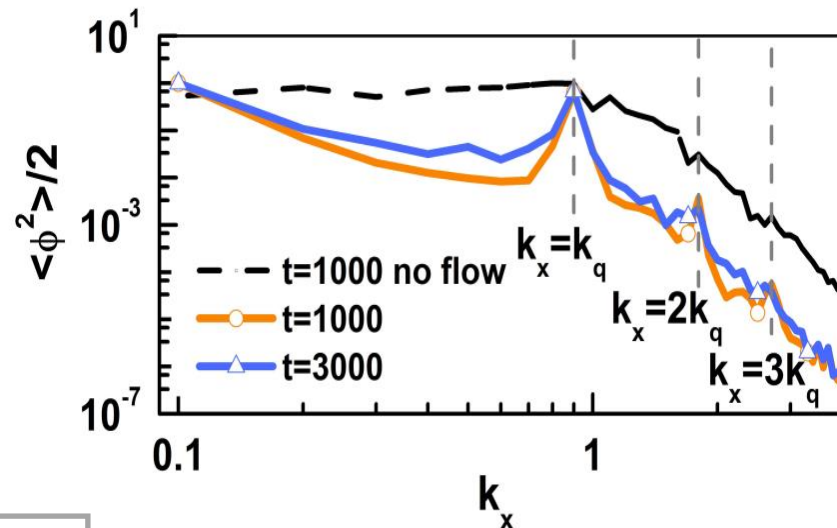
✓ Evolution of potential energy spectrum

Preparing for the future

• Spectrum of k_y



• Spectrum of k_x



Mode coupling

- **Critical ITG instability** $k_y = 0.7 \sim 0.8$
- **Coupling with** $k_y = 0.1$
- **Secondary instability** $k_y = 0.8 \sim 0.9$

- **The peaks of poloidal spectrum emerge.**
- **The radial spectral peaks disappear.**

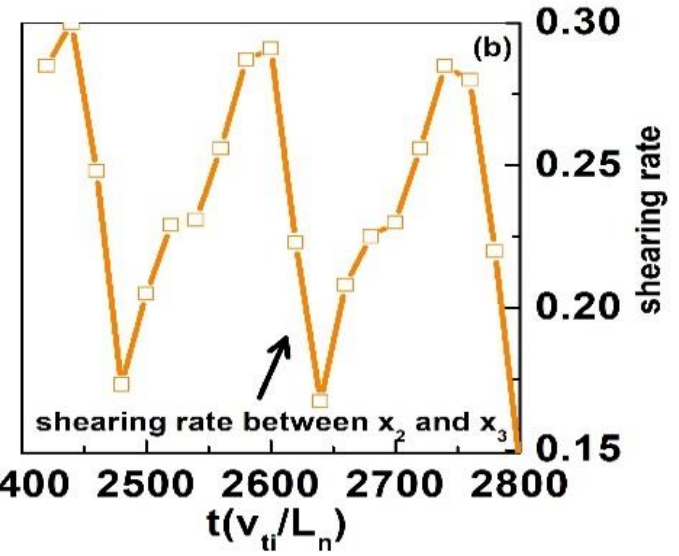
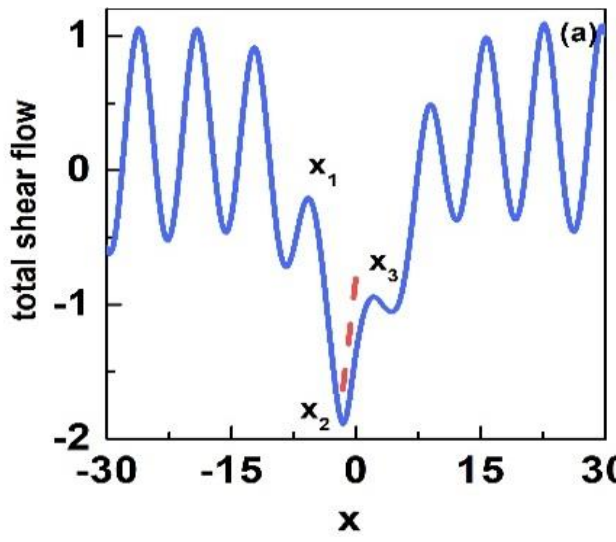
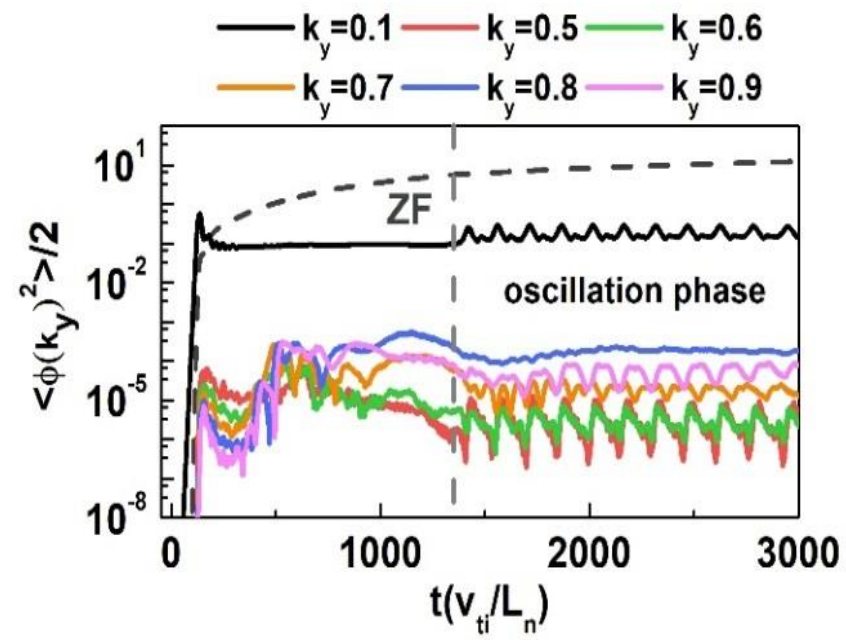
✓ Effect of the imposed shear flows

Preparing for the future

• Zonal flow & KH instability & ITG instability

($A = 0.9$)

• Evolution of shear flows



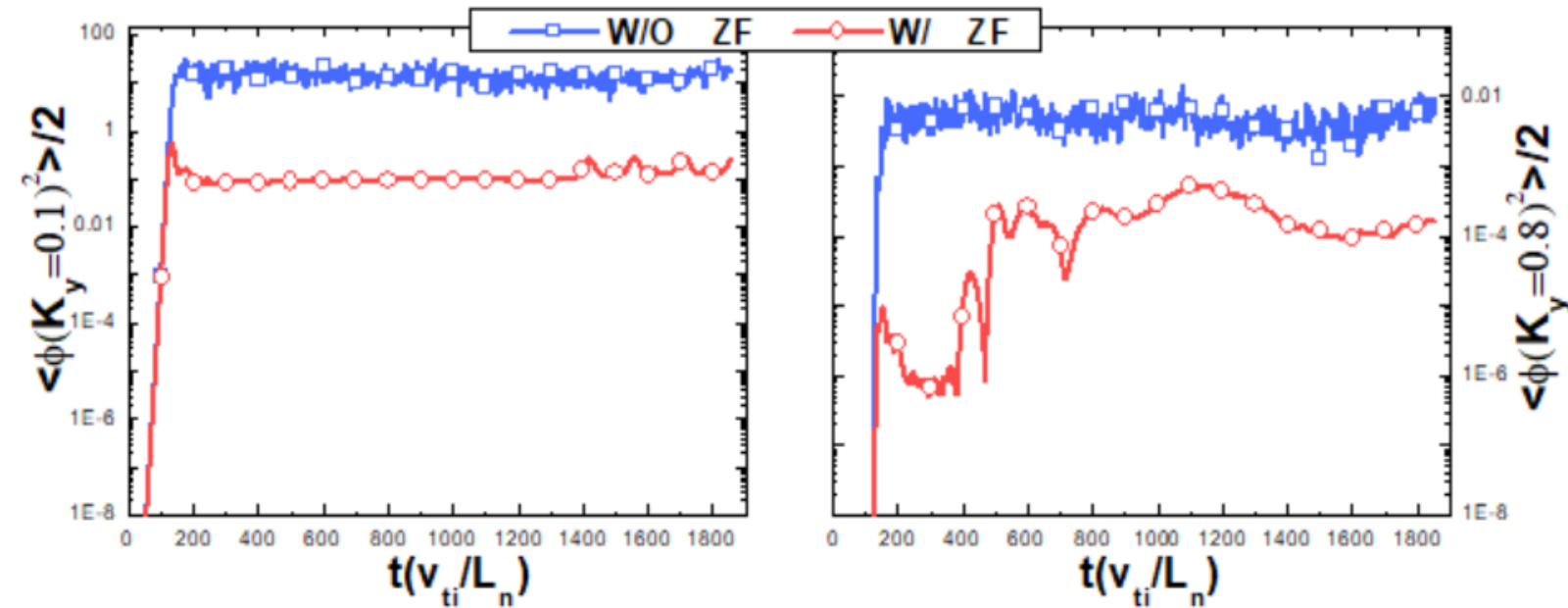
- $k_y = 0.9$: **without oscillating** after coupling;
- $k_y = 0.8$: **oscillate**;
- Energy of $k_y = 0.1$ transfers to $k_y = 0.9$.

- Velocity difference: **oscillating**;
- Same to oscillation behavior of $k_y = 0.1$.

✓ Roles of Zonal flow

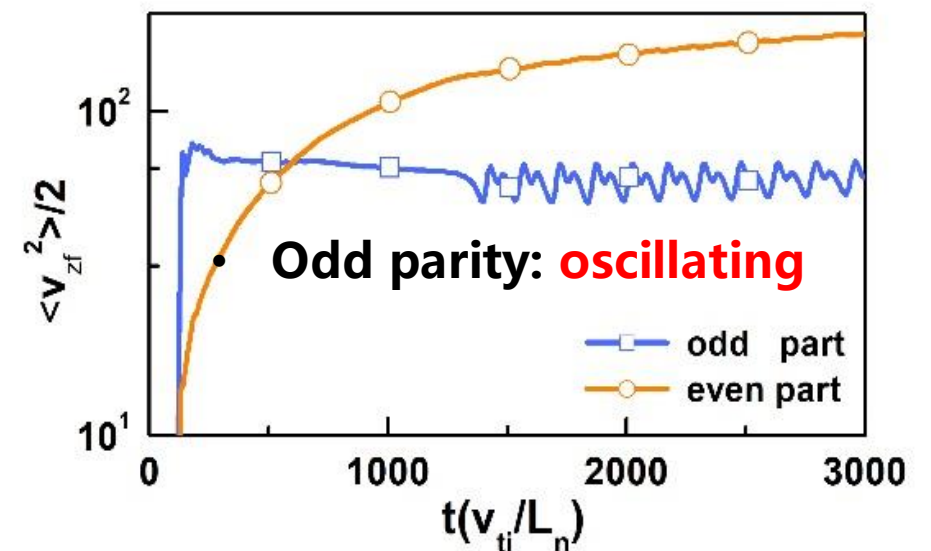
Preparing for the future

• Evolution of energy with or without ZF



- The **oscillations disappear**;
- The energy increasement of ITG **vanishes**.

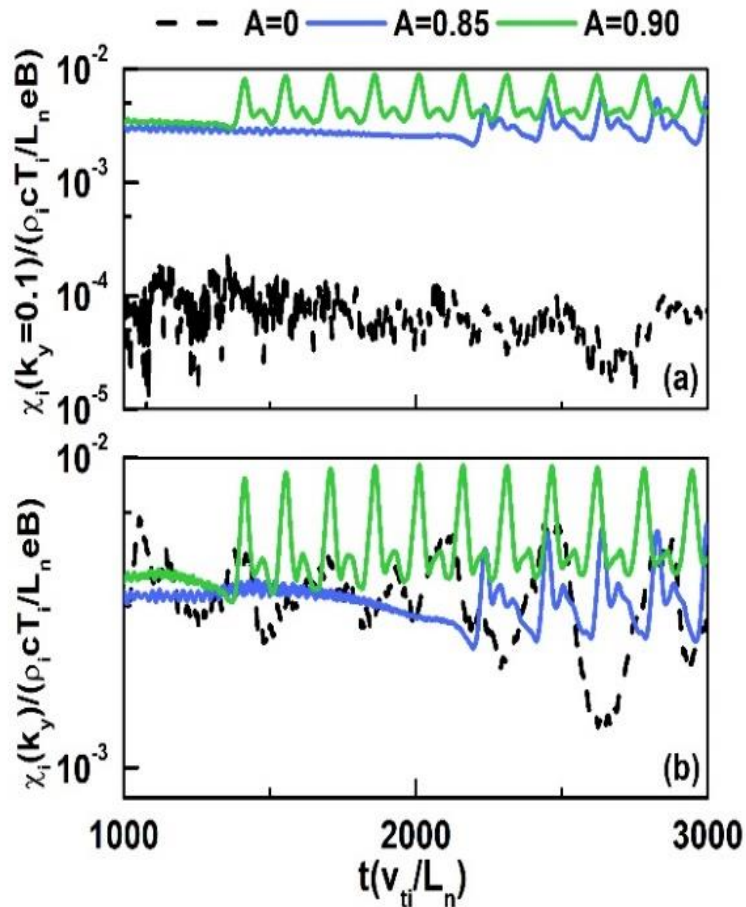
• Even and odd parity of ZF



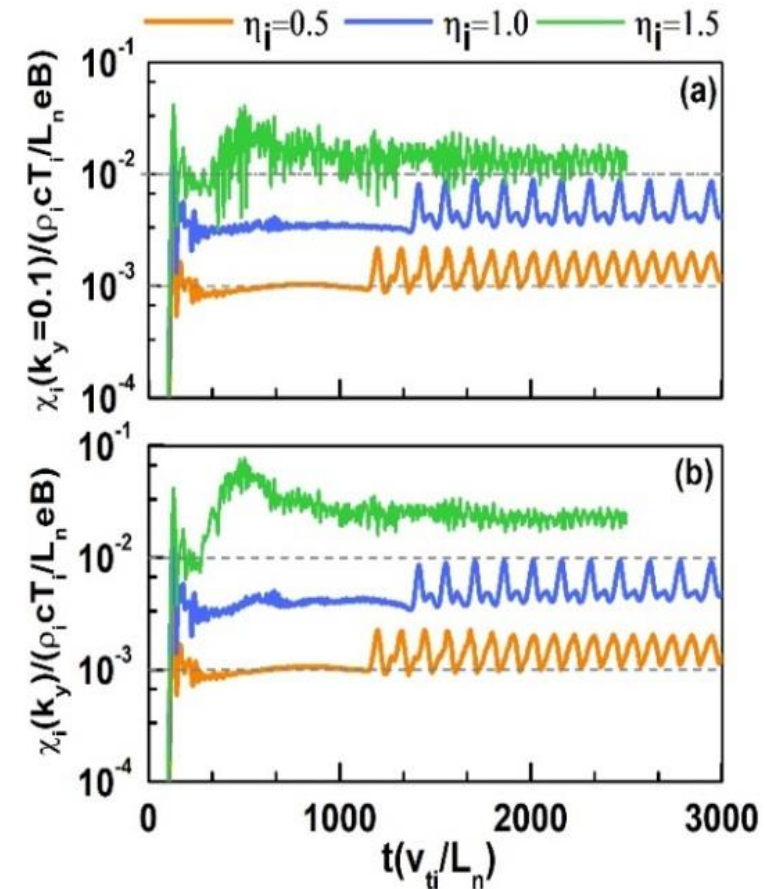
✓ Ion heat transport

Preparing for the future

• Ion heat transport with various A



• Ion heat transport with various η_i



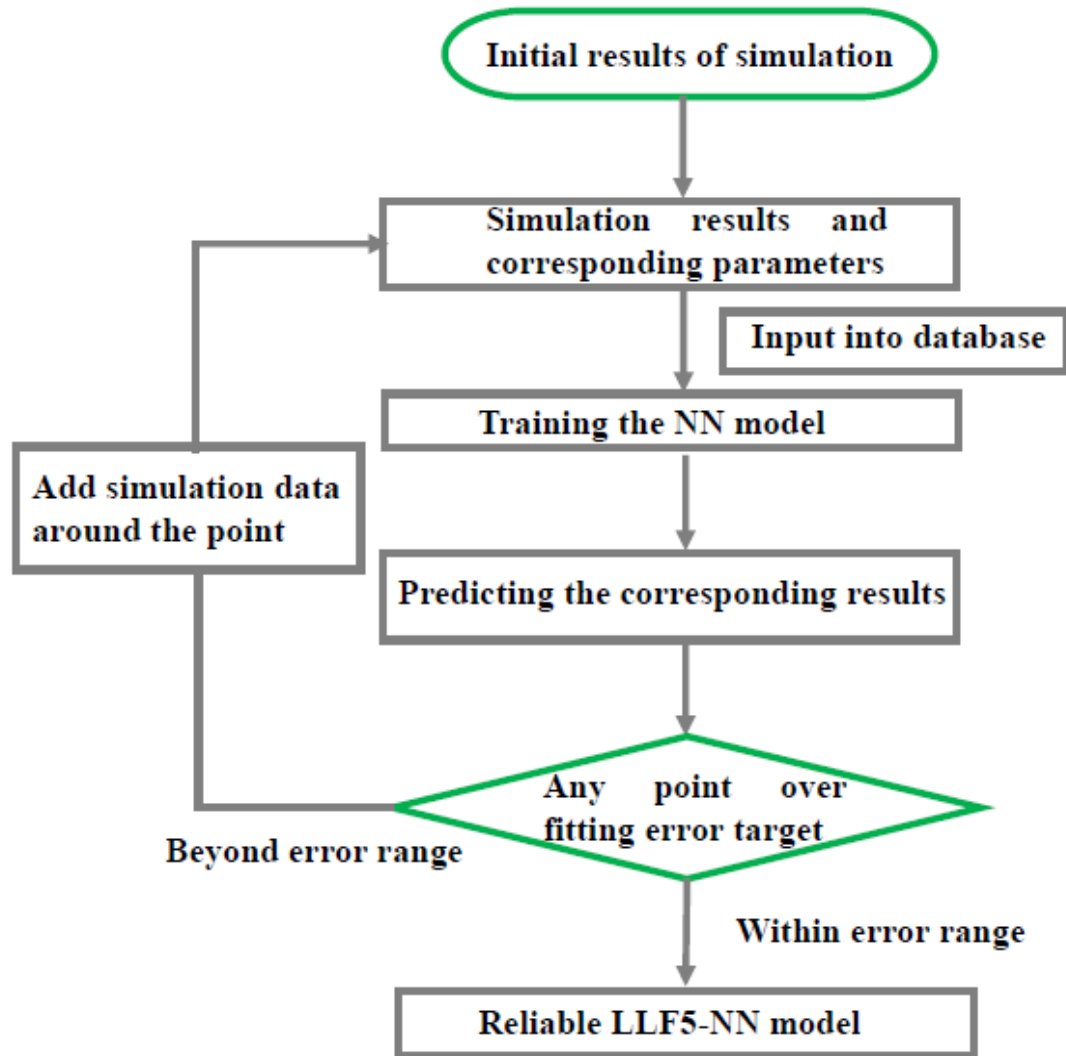
Hui Li, J. Q. Li, Z. X. Wang, L. Wei, et al. *Phys. Plasmas* 27, 082304 (2020).

Hui Li, J. Q. Li, Z. X. Wang, L. Wei, et al. *Chin. Phys. B* 31, 065207 (2022).

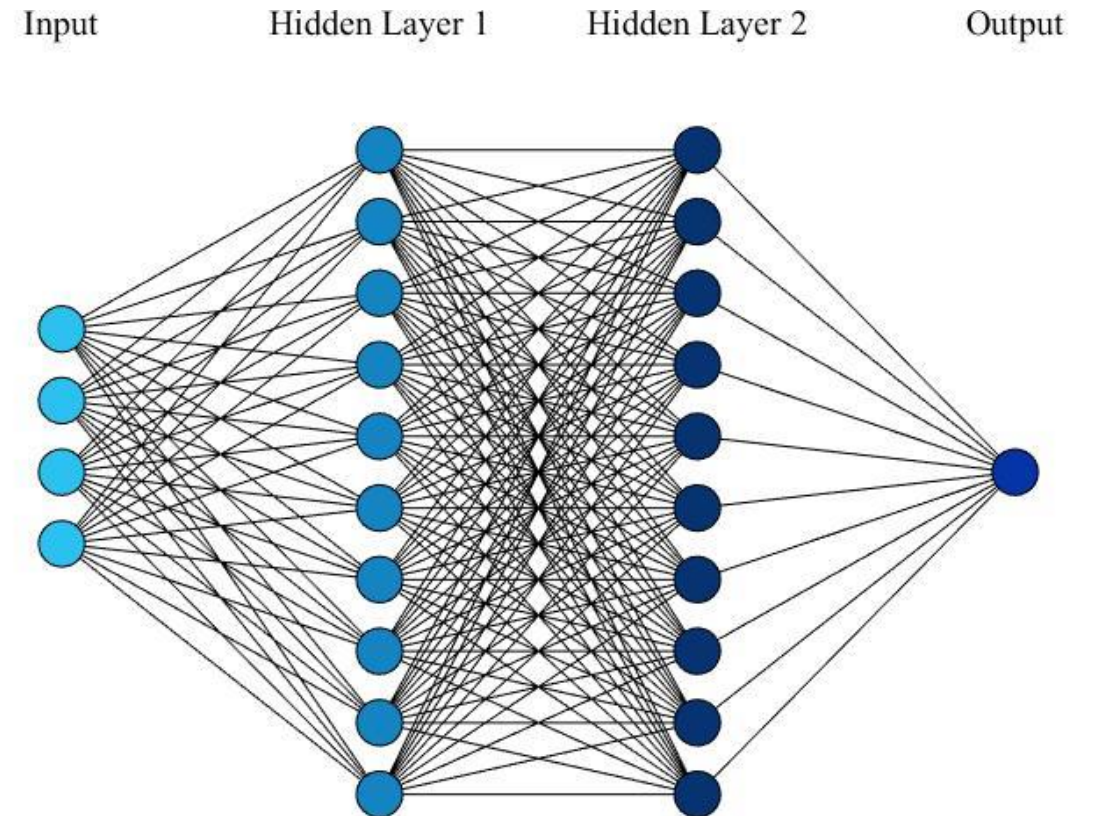
✓ Construction of LLF5-NN

Preparing for the future

• Schematic diagram of LLF5-NN

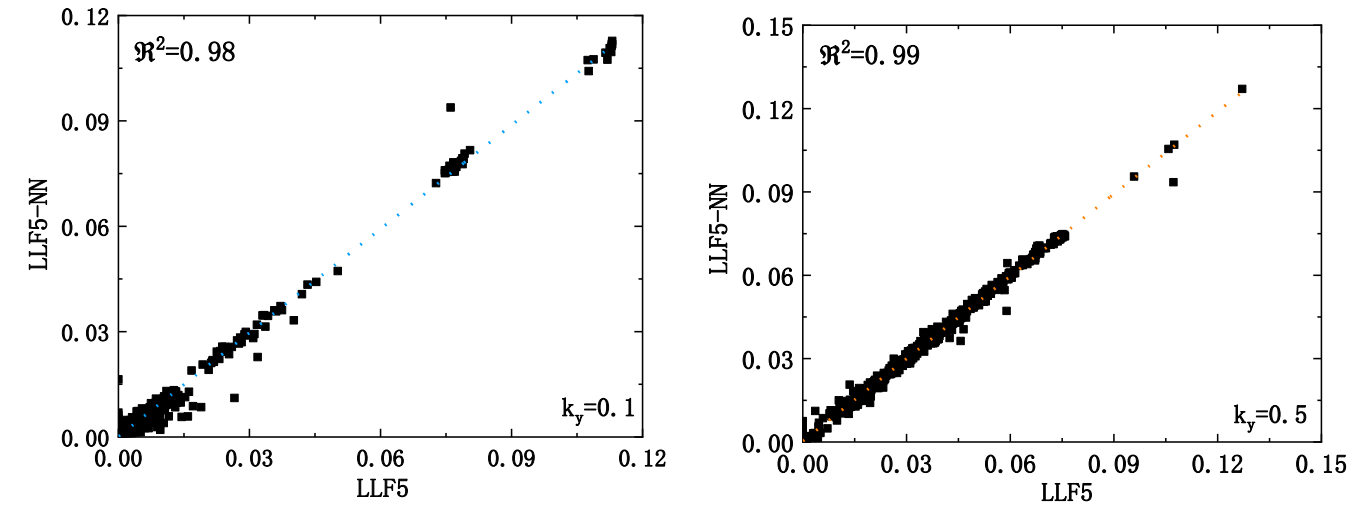


• NN topology



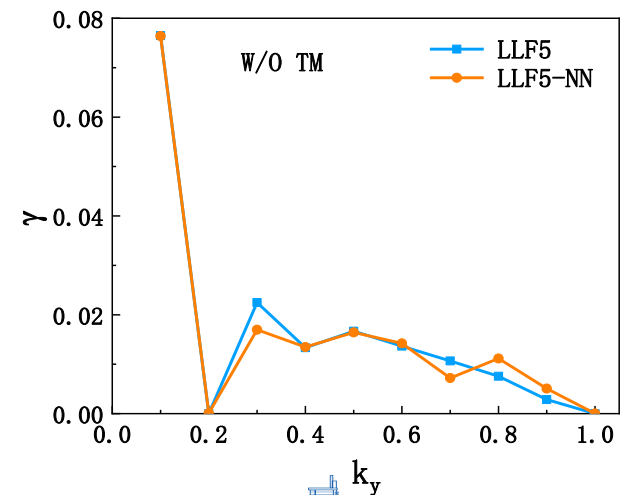
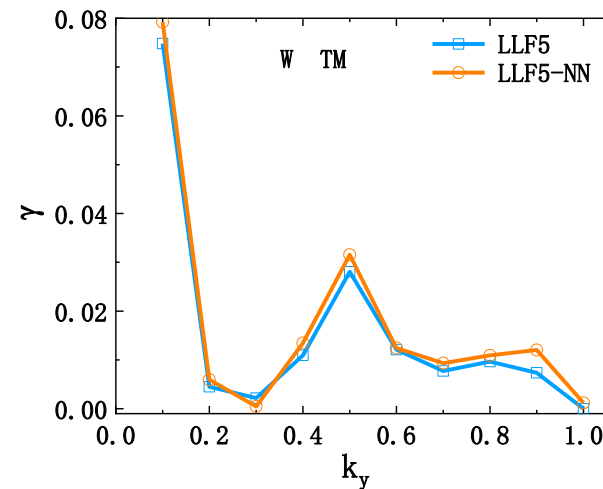
✓ Prediction of growth rate spectrum

Preparing for the future



• Spectrum of growth rates

• Regression histograms

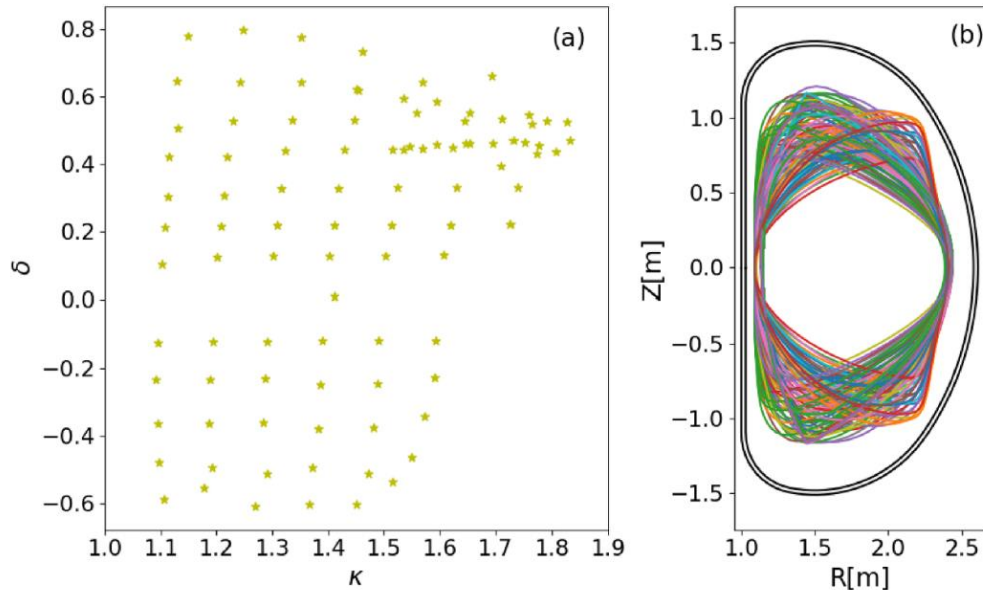


► Neural network based fast prediction of β_N limits in HL-2M

Preparing for the future

- Operational scenarios: HL-2M;
- Neural networks are trained, based on the numerical database, to predict no-wall and ideal-wall β_N limits
- Database: lower single null and double-null divertor configurations;
- Limiter configurations: positive and negative triangularity plasmas.

• Plasma boundary shaping

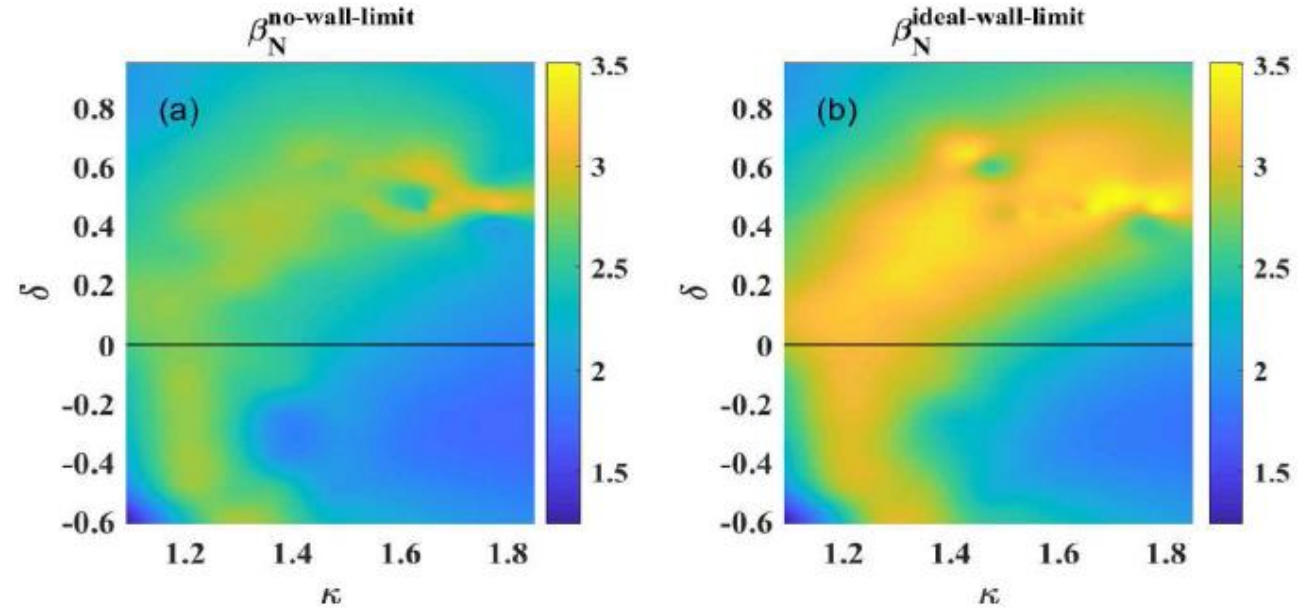
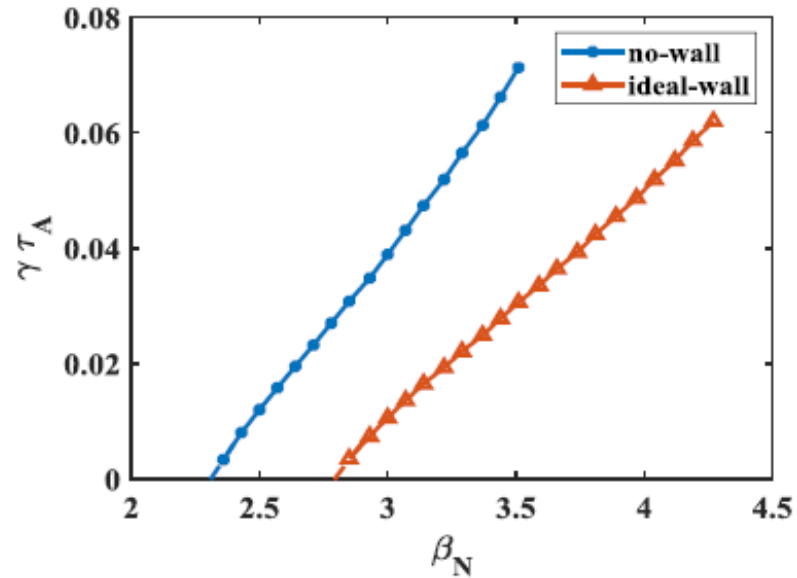


- (a): triangularity and elongation distribution
- (b): all boundary shapes plotted together with modeled double-wall structure in HL-2M.

Neural network based fast prediction of β_N limits in HL-2M

Preparing for the future

- Simulation results are displayed.
- MARS-F computes growth rate of ideal external kink instability.

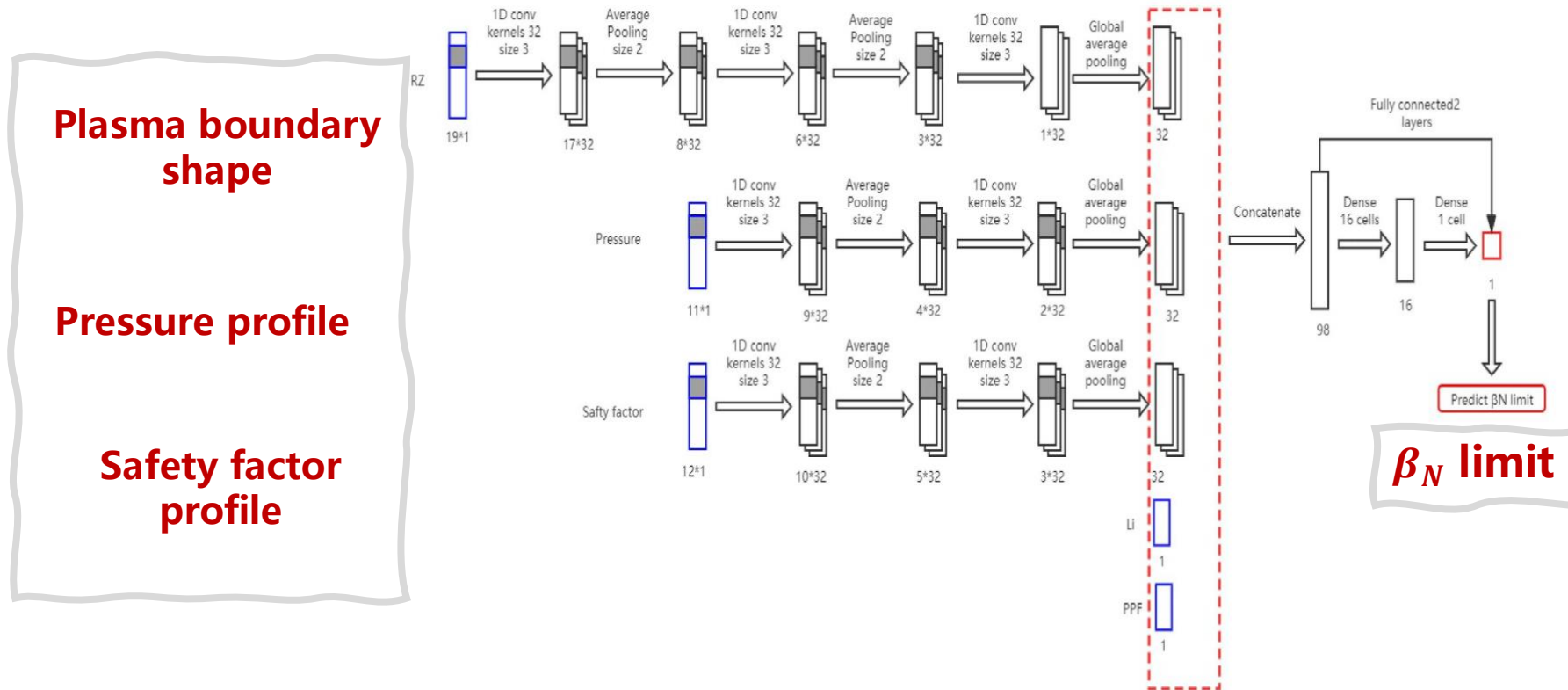


- MARS-F computed no-wall and ideal wall β_N limits;
- Varying both triangularity and elongation of plasma boundary shape;
- Both β_N limits increase with the plasma elongation, being consistent with the previous finding.

Neural network based fast prediction of β_N limits in HL-2M

Preparing for the future

- Structure for CNN (Convolutional Neural Network)



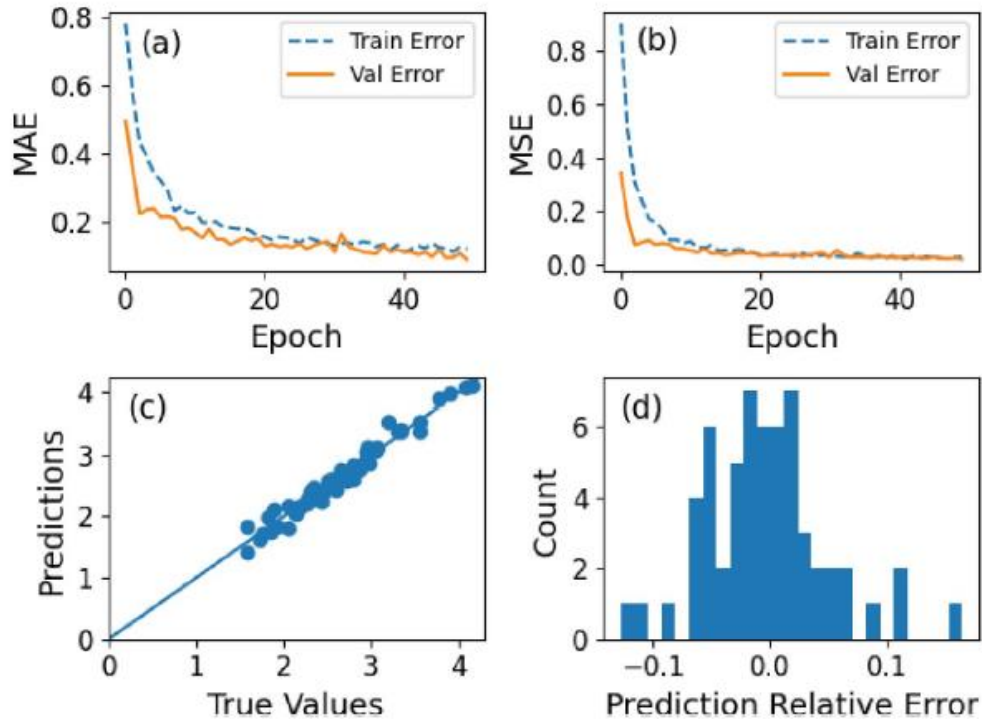
- CNN is considered and composed of five parts.
- Three input types.
- It aims at predicting β_N limit which is a real positive number.



Neural network based fast prediction of β_N limits in HL-2M

Preparing for the future

• Training results for n=1 no-wall



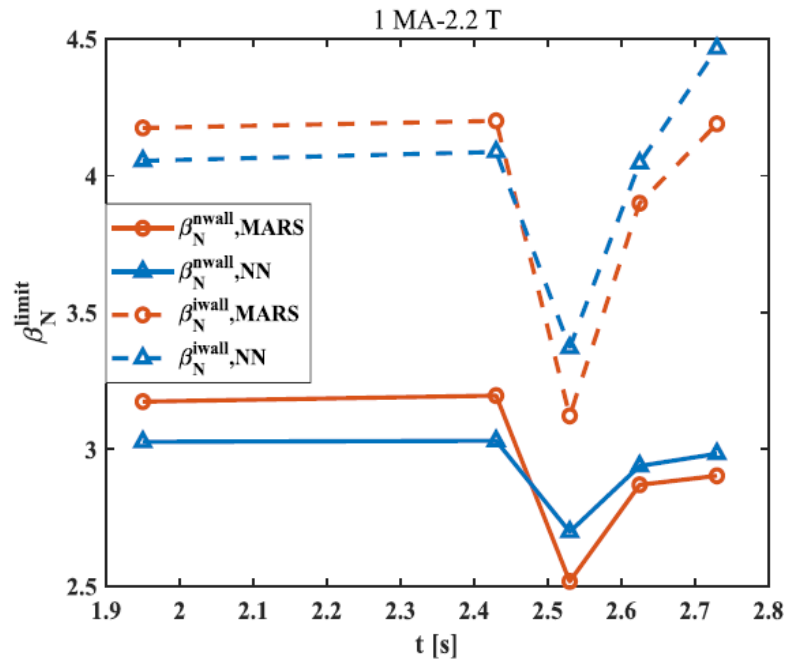
- CNN training and testing results for n=1 no-wall β_N limit.
- (a), (b) are mean absolute error and mean square error, versus training epoch for both training set and validation set.
- (c) are CNN-predicted β_N limits versus MARS-F computed values labeled as 'True Values' along horizontal axis, for testing dataset.
- (d) reports the number of sample counts versus relative error.

- (a): mean absolute error (MAE)
- (b): mean square error (MSE)
- (c): CNN-predicted vs MARS-F computed
- (d): sample counts vs relative error MARS-F and CNN

Neural network based fast prediction of β_N limits in HL-2M

Preparing for the future

- Compared btw CNN and MARS-F



- MARS-F computed and CNN-predicted β_N limits, again for testing dataset.
- Compared to direct results computed by MARS-F, CNNs consistently perform well in predicting both limits, not only in general trends but also in quantitative values.

It can be used as a real-time monitor for disruption prevention in HL-2M, or serve as part of integrated modeling tools for ideal β_N limits



1

Background & Motivation

2

Multi-mode interaction & Neural network

3

Multi-scale interaction & Neural network

4

Summary

CONTENT

► Micro-instability/ Macro-instability & Machine Learning

Preparing for the future

• Two models

ExFC-NN>

Dominant type of turbulence

Radial averaged fluxes

Radial perturbation and fluxes

Experimental process

Time evolution of flux

SGL5>

Growth rate spectrum

Transport coefficient

Pattern Recognition

Energy evolution

Transport coefficient evolution

• Neural network based fast prediction of β_N limits in HL-2M

- Hui Li, J. Q. Li, Y. L. Fu, Z. X. Wang, *et al.* *Nucl. Fusion* 62, 036014 (2022).
- Hui Li, Y. L. Fu, J. Q. Li, Z. X. Wang. *Plasma Sci. Technol.* 23, 115102 (2021).
- Hui Li, J. Q. Li, Z. X. Wang, L. Wei, *et al.* *Phys. Plasmas* 27, 082304 (2020).
- Hui Li, J. Q. Li, Z. X. Wang, L. Wei, *et al.* *Chin. Phys. B* 31, 065207 (2022).
- Hui Li, J. Q. Li, Z. X. Wang, L. Wei, *et al.* *Chin. Phys. B* 32, 075206 (2023).
- Hui Li, *et al.* *Chinese Physics Letters* 40, accepted (2023)
- Hui Li, *et al.* *Chinese Physics Letters* 40, 105201 (2023)
- T. Liu, Hui Li, *et al.* *iEnergy* 1, 2 (2022).
- X. L. Zhu, Hui Li, *et al.* *iEnergy* 1, 3 (2022).
- Y. F. Zhao, *et al.* *Plasma Phys. Controlled Fusion* 64, 4 (2022).

